effect of the oxygens bonded directly to the two carbons. The absence of this band from the SERS spectrum suggests immediately that the oxalate ion lies down on the silver surface. The band at 892 cm^{-1} is therefore assigned to the COO^- deformation which comes at 904 cm^{-1} in solution.[9] For the other carboxylate ions this vibration is found near 670 cm^{-1} in solution. It is not seen in the SERS spectra of the other carboxylates partly because these modes are inherently weak and partly because, unlike the oxalate ion, the carboxylate groups of the other acids stand up on the surface, at least partially, as in Figure 3.

Acknowledgment. We thank NSERC and the donors of the petroleum research fund, administered by the American Chemical Society, for partial support for this work.

Registry No. Valeric acid, 109-52-4; hexanoic acid, 1289-40-3; heptanoic acid, 111-14-8; octanoic acid, 124-07-2; nonanoic acid, 112-05-0; decanoic acid, 334-48-5; oxalic acid, 144-62-7; succinic acid, 110-15-6; glutaric acid, 110-94-1; adipic acid, 124-04-9; pimelic acid, 111-16-0; suberic acid, 505-48-6; silver, 7440-22-4.

(9) Ito, K.; Bernstein, H. J. *Can. J. Chem.* **1956**, *34*, 170.

Haptotropic Rearrangements in Polyene–ML_n Complexes. 3. Polyene–ML_2 Systems

Jerome Silvestre[1a] **and Thomas A. Albright***[1b]

Contribution from the Department of Chemistry, University of Houston, Houston, Texas 77004. *Received April 22, 1985*

Abstract: A general theoretical study has been undertaken for the rearrangement of an ML_2 group from one coordination site to another in polyene–ML_2 complexes. Extended Hückel calculations have been used to compute the minimum energy reaction pathways in the U, sickle, and W isomers of pentadienyl–$Pt(PH_3)_2^+$, benzyl–$Rh(PH_3)_2$, phenalenium–$Pt(PH_3)_2^+$, quinone–$Pt(PH_3)_2$, fulvene–$Pt(PH_3)_2$, cyclobutadiene–$Ni(PH_3)_2$, benzene–$Ni(CO)_2$, and cyclopentadienyl–$Pt(CO)_2^-$. A simple, topologically based model is developed to analyze these and other rearrangements. For a d^{10} complex, it maximizes overlap between the ML_2 b_1 orbital and the LUMO of the polyene along the reaction path. For a d^8 complex, the polyene HOMO is used in an analogous fashion. The method is in good agreement with detailed computations for all systems, except benzene–$Ni(CO)_2$. Here superjacent orbital control determines the geometry of the transition state. A qualitative estimate of the activation energy for the rearrangement can be determined by establishing how much overlap between the ML_2 b_1 orbital and requisite polyene π orbital is lost on going from the ground to transition state. Repulsion between the filled ML_2 b_2 and a filled polyene π orbital can also contribute to the barrier. It is shown how perturbation of the electronic properties in the auxiliary ligands at the metal can modify this repulsion and the associated activation energy.

Introduction

Haptotropic rearrangements, wherein a ML_n unit changes its connectivity (hapto number) to some ligand with multicoordination site possibilities, has been extensively studied by experiment[2] and theory[3] for polyene–ML_3 and –MCp systems. Far less is known[2c] about polyene–ML_2 complexes, although there have been prior theoretical studies of fluxionality in η^3-cyclohexadienyl–ML_2 and η^2-cyclopropenium–ML_2^+ compounds.[4] In this work, we present a general theoretical strategy that can be readily used for analyzing haptotropic rearrangements in polyene–ML_2 complexes. We have also generated potential energy surfaces with the aid of molecular orbital calculations at the extended Hückel level[5] to check our theoretical model.

Haptotropic rearrangements in 16-electron benzyl–ML_2 complexes nicely illustrate some of our concerns. The compounds undergo a very facile rearrangement shown in **1**. While a π–σ–π

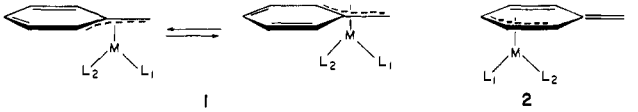

1 2

route has been commonly proposed for fluxionality in benzyl–ML_n complexes,[7] this mechanism has been conclusively proven in only

(1) (a) Current address: Department of Chemistry, Cornell University, Ithaca, NY 14853. (b) Camille and Henry Dreyfus Teacher-Scholar, 1980–1984; Alfred P. Sloan Research Fellow, 1982–1986.

(2) For leading reviews, see: (a) Cotton, F. A. "Dynamic Nuclear Magnetic Resonance Spectroscopy"; Jackman, L. M., Cotton, F. A., Eds.; Academic Press: New York, 1975; Chapter 10. (b) Faller, J. W. *Adv. Organomet. Chem.* **1977**, *16*, 211. (c) Mann, B. E. "Comprehensive Organometallic Chemistry"; Wilkinson, G., Stone, F. G. A., Abel, E. W., Eds.; Pergammon Press: Oxford, 1982; Vol. 3, pp 89–71. (d) Deganello, G. "Transition Metal Complexes of Cyclic Polyolefins"; Academic Press: New York, 1979. (e) Fedorov, L. A. *Russ. Chem. Rev.* **1973**, *42*, 678.

(3) (a) Albright, T. A.; Hofmann, P.; Hoffmann, R.; Lillya, C. P.; Dobosh, P. A. *J. Am. Chem. Soc.* **1983**, *105*, 3396. (b) Hofmann, P.; Albright, T. A. *Angew. Chem.* **1980**, *92*, 747; *Angew. Chem., Int. Ed. Engl.* **1980**, *19*, 728. (c) Albright, T. A.; Geiger, W. E., Jr.; Moraczewski, J.; Tulyathan, B. *J. Am. Chem. Soc.* **1981**, *103*, 4787. (d) Herndon, W. C. *Ibid.* **1980**, *102*, 1538. (e) Karel, K. J.; Albright, T. A.; Brookhart, M. *Organometallics* **1982**, *1*, 419. (f) Mingos, D. M. P. *J. Chem. Soc., Dalton Trans.* **1977**, 31.

(4) (a) Mealli, C.; Midollini, S.; Moneti, S.; Sacconi, L.; Silvestre, J.; Albright, T. A. *J. Am. Chem. Soc.* **1982**, *104*, 95. (b) Albright, T. A.; Hoffmann, R.; Yse, T.-Y.; D'Ottavio, T. *Ibid* **1979**, *101*, 3812. (c) Mingos, D. M. P.; Nurse, C. R. *J. Organomet. Chem.* **1980**, *184*, 281.

(5) Hoffmann, R.; Lipscomb, W. N. *J. Chem. Phys.* **1962**, *36*, 2179, 3489; **1962**, *37*, 2872. Hoffmann, R. *Ibid.* **1963**, *39*, 1397.

(6) (a) Sonoda, A.; Mann, B. E.; Maitlis, P. M. *J. Chem. Soc., Chem. Commun.* **1975**, 108. (b) Mann, B. E.; Keasey, A.; Sonoda, A.; Maitlis, P. M. *J. Chem. Soc., Dalton Trans.* **1979**, 338. (c) Sonoda, A.; Bailey, P. M.; Maitlis, P. M. *Ibid* **1979**, 346. (d) Burch, R. R.; Muetterties, E. L.; Day, V. W. *Organometallics* **1982**, *1*, 188. (e) Becker, Y.; Stille, J. K. *J. Am. Chem. Soc.* **1978**, *100*, 845. (f) Roberts, J. S.; Klabunde, K. J. *Ibid.* **1977**, *99*, 2509. (g) Stühler, H.-O.; Pickardt, J. *Z. Naturforsch.*, **1981**, *36B*, 316. See also: Stühler, H.-O. *Angew. Chem.* **1980**, *92*, 475; *Angew. Chem., Int. Ed. Engl.* **1980**, *19*, 468.

(7) (a) Tsutsui, M.; Courtney, A. *Adv. Organomet. Chem.* **1977**, *16*, 241. Gorewit, B.; Tsutsui, M. *Adv. Cataly.* **1978**, *27*, 227. (b) Muetterties, E. L.; Hirsekorn, F. J. *J. Am. Chem. Soc.* **1973**, *95*, 5419; **1974**, *96*, 7920. Bleeke, J. R.; Burch, R. R.; Coulman, C. L.; Schardt, B. C. *Inorg. Chem.* **1981**, *20*, 1316. (c) Bennett, M. A.; McMahon, I. J.; Turney, T. W. *Angew. Chem.* **1982**, *92*, 273; *Angew. Chem., Int. Ed. Engl.* **1982**, *21*, 379. (d) Cotton, F. A.; Marks, T. J. *J. Am. Chem. Soc.* **1969**, *91*, 1339. Cotton, F. A.; LaPrade, M. D. *Ibid* **1968**, *90*, 5418. (e) King, R. B.; Fronzaglia, F. *Ibid.* **1966**, *88*, 709.

0002-7863/85/1507-6829$01.50/0

one case (in the presence of a noncoordinating solvent).[7d] Indeed, Mann and co-workers[6a,b] have devised an elegant NMR experiment utilizing trityl–ML_2 complexes which convincingly demonstrates that a $\pi-\sigma-\pi$ route is *not* a low-energy process for the rearrangement in **1**. Further NMR experiments[6a,b,d] have shown that the auxiliary ligand L_1 in **1** remains cis to the exocyclic methylene group (and L_2 remains trans) during the rearrangement in these pseudosquare-planar complexes.. A least-motion path where the ML_2 unit migrates from one side of the benzyl ligand to the other has been proposed[6b] for **1**. Muetterties and co-workers[6d] have suggested an alternative route in which the ML_2 unit migrates to an endocyclic η^3 (or η^5) intermediate, **2**. Can one then differentiate between these two reaction pathways? Ring whizzing, wherein a ML_n group migrates inside the periphery of a cyclic polyene, is a common type of haptotropic rearrangement which normally proceeds with a low-to-moderate energy barrier.[2] We have previously shown[4a] that the activation energy for ring whizzing in cyclopropenium–$M(PPh_3)_2^+$ complexes (M = Ni, Pd, and Pt), **3**, is very small. Changing the metal or even counteranion

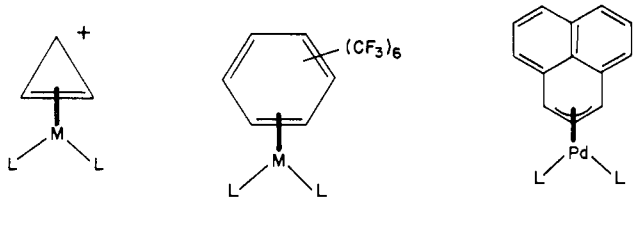

3 **4** **5**

causes the structure of the molecule in the solid state to vary, so the reaction path for ring whizzing could be charted by X-ray structures. The activation energy associated with this system must be less than 5 kcal–mol.[4a] Stone and co-workers have prepared a number of hexakis(trifluoromethyl)benzene–ML_2 complexes[8] where M = Ni(0) and Pt(0), **4**. The barrier for the $Pt(PEt_3)_2$ complex was estimated to be ~11 kcal/mol.[8a] The activation energy for ring whizzing in phenalenium–ML_2 compounds[9] must be substantially higher. For example, in **5** (L_2 = acac), there was no evidence for fluxionality in ^1H NMR studies up to +60 °C which implies that $\Delta G^{\ddagger} > \sim 18$ kcal/mol.[9a] Thus, there is a sizable range of activation energies that are encountered for these haptotropic rearrangements. Furthermore, the ML_2 unit may undergo a simple sliding motion or it may rotate as it shifts from one coordination site to another. A model to analyze haptotropic rearrangements should be able to differentiate reaction paths and associated stereochemical modes, as well as to offer a qualitative estimate of the activation energy. Such a topologically based model is developed in the next section.

General Theoretical Strategy

A natural way to analyze haptotropic rearrangements is to examine how the overlap changes between the valence orbitals of a ML_2 unit and the π orbitals of the polyene on going from the ground to transition state. The valence orbitals of a ML_2 fragment are displayed in Figure 1. These orbitals have been derived elsewhere;[10] therefore, only a brief description is given

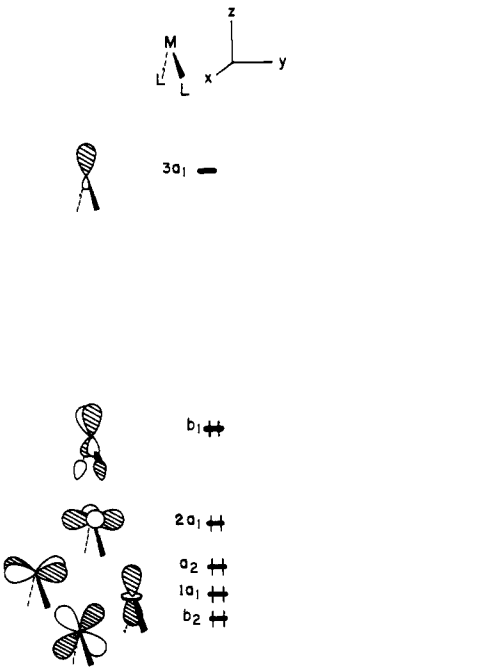

Figure 1. Valence orbitals of a ML_2 fragment with C_{2v} symmetry. The electron occupancy shown is for a d^{10} complex.

here. At low energy is a nest of four orbitals, $b_2 + 1a_1 + a_2 + 2a_1$. They are highly localized on the metal and are primarily of d character. At higher energy, the b_1 orbital is metal *xz* mixed in a antibonding manner with the lone pair functions at the ligands. Furthermore, metal *x* mixes into b_1 so that the orbital is hybridized away from the auxiliary ligands (toward the polyene in a polyene–ML_2 complex). Finally, at still higher energy the $3a_1$ orbital is primarily a metal s and *z* hybrid. In an arbitrary polyene–ML_2 complex, the $2a_1$ and a_2 levels of ML_2 have δ symmetry with respect to the polyene. Therefore, not much overlap between them and the π orbitals will exist. The $1a_1$ and $3a_1$ orbitals interact in a σ fashion. They will have the largest overlap with a polyene π orbital containing few nodal planes, most commonly the *lowest* π orbital. This leaves us with the b_1 and b_2 fragment orbitals. The majority of the systems that we shall investigate can be partitioned into a d^{10} ML_2 fragment interacting with a polyene. Both b_1 and b_2 may be stabilized by interaction with unfilled polyene π^* orbitals. However, the stabilization of b_1 will be larger than that associated with b_2. First of all, the b_1 level lies at a higher energy than b_2 does; therefore, the energy gap between b_1 and the empty π^* orbital will be less than that between b_2 and π^*. Second, b_1 is hybridized toward the polyene, whereas b_2 is not. This leads to a larger $b_1-\pi^*$ overlap than that between b_2 and π^*. From these considerations, one can then generalize that the leading source of bonding in a d^{10} polyene–ML_2 complex will be derived from the interaction between the b_1 HOMO of ML_2 and the lowest unoccupied π orbital of the polyene.

An alternative, perhaps more simple, way to derive the orbital pattern for ML_2 is to consider the perturbation encountered when two cis ligands are removed from a d^8 square-planar ML_4 complex. Two vacant orbitals at the metal are created which point toward the two missing ligands, **6**. Symmetry-adapted linear combi-

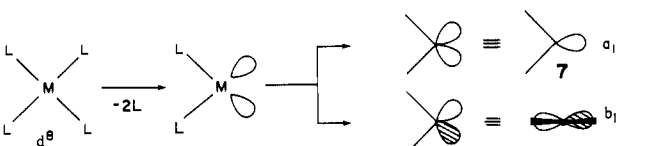

nations of these two hybrid orbitals generate one orbital of a_1 symmetry, **7**, which is analogous to $3a_1$ in Figure 1. The antisymmetric combination of **6** yields the b_1 orbital, **8**. A convenient bottom view of this orbital which we shall use extensively is shown

(8) (a) Browning, J.; Green, M.; Penfold, B. R.; Spencer, J. L.; Stone, F. G. A. *J. Chem. Soc., Chem. Commun.* **1973**, 31. (b) Browning, J.; Cundy, C. S.; Green, M.; Stone, F. G. A. *J. Chem. Soc. A* **1971**, 448. (c) Browning, J.; Green, M.; Spencer, J. L.; Stone, F. G. A. *J. Chem. Soc., Dalton Trans.* **1974**, 97. (d) Browning, J.; Penfold, B. R. *J.Cryst. Mol. Struct.* **1974**, *4*, 335.

(9) (a) Nakasuji, K.; Yamaguchi, M.; Murata, I.; Tatsumi, K.; Nakamuri, A. *Organometallics* **1984**, *3*, 1257; *Chem. Lett.* **1983**, 1489. (b) Keasey, A.; Bailey, P. M.; Maitlis, P. M. *J. Chem. Soc., Chem. Commun.* **1978**, 142. (c) Lin, S.; Boudjouk, P. *J. Organomet. Chem.* **1980**, *187*, C11.

(10) (a) Radonovich, L. J.; Koch, F. J.; Albright, T. A. *Inorg. Chem.* **1980**, *19*, 3373. (b) Byers, L. R.; Dahl, L. F. *Ibid.* **1980**, *19*, 277. (c) Albright, T. A.; Hoffmann, R. *Chem. Ber.* **1978**, *111*, 1578. (d) Mingos, D. M. P.; Forsyth, M. J.; Welch, A. *J. Chem. Soc., Dalton Trans.* **1978**, 1363. Mingos, D. M. P. *Ibid* **1978**, 602. (e) Albright, T. A.; Hoffmann, R.; Thibeault, J. C.; Thorn, D. L. *J. Am. Chem. Soc.* **1979**, *101*, 3801. (f) Burdett, J. K. *Inorg. Chem.* **1975**, *14*, 375; *J. Chem. Soc., Faraday Trans. 2* **1974**, *70*, 1599. (g) Hofmann, P. *Angew. Chem.* **1977**, *89*, 551. Habilitationshricft, University of Erlangen, 1978.

by **9**. The reader can easily verify that the remaining ML_2 orbitals in Figure 1 correspond to the filled orbitals in a classical square-planar splitting pattern. Now for a d^{10} system, the b_1 orbital is filled and a_1 (**7**) is empty. These two orbitals will form the dominant bonding interaction to a polyene. As stated previously, a_1 interacts most strongly with the lowest-occupied π level in a polyene. Since this is the fully bonding combination of polyene p orbitals, the overlap between it and a_1 is not particularly sensitive to where the ML_2 unit lies with respect to the polyene. This is certainly not the case for the interaction between filled b_1 (**9**) and the LUMO of a polyene. As we shall see below, it is this interaction which determines the reaction path and the stereochemistry associated with the haptotropic rearrangement, i.e., whether the ML_2 rotates or slides as it shifts from one coordination site to another. The details of the reaction path are governed by maximizing the overlap between b_1 and the LUMO of the polyene. Likewise, the amount of energy associated with the reaction path can be estimated in a very qualitative sense by noting how much overlap is lost between b_1 and the polyene LUMO on going from the ground to transition state. We emphasize that the actual magnitude of the activation energy cannot be determined by using this approach; that will depend strongly on the exact nature of the ML_2 group. In other words, if the binding energy of ML_2 to the polyene is small in the ground state, then although a large amount of the b_1–π^* overlap may be lost at the transition state, the corresponding activation energy will be relatively small.

The interested reader should note that we have singled out one orbital in ML_2 which sets the reaction path for haptotropic rearrangements in polyene complexes. For a ML_3 or MCp complex, there are *two* orbitals, **10**, which are utilized in an analogous fashion.[3a] Since d^{10} ML_2 and d^8 ML_4 fragments are isolobal,[11]

10

the arguments that we make here concerning d^{10} polyene–ML_2 complexes apply equally well to d^8 polyene–ML_4 systems. In the latter case, the reaction paths and energetics are determined by the interaction of **11**, which is occupied, with the LUMO of the polyene. Finally, Mingos has used[3f] an alternative model to view

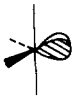

11

ring-whizzing in **4**. His method relies on the formulation of a metal–polyene bonding network and an associated basis set of orbitals. A decision can then be made for whether bonds are broken in a superfacial or antarafacial manner and the generalized Woodward–Hoffmann rules can be applied to determine if the reaction path is allowed or forbidden. It should be emphasized that there is a close correspondence between our and Mingos' method. They will always lead to identical results. Both models are based on the assumption of effective square-planar coordination at the metal atom and hence to the dominance of the metal b_1–polyene π interaction.

η^3-Pentadienyl–ML_2 Complexes

There are three isomeric, 16-electron η^3-pentadienyl–ML_2 complexes which can undergo haptotropic rearrangements. These are shown in **12–14** for the W, sickle, and U isomers, respectively. Since these three basic patterns can be readily extended to other situations, we shall spend some time on their analysis. In each

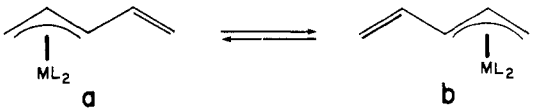

12

13

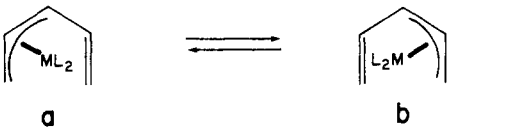

14

case, the molecule can be partitioned into a d^{10} ML_2 unit interacting with a pentadienyl cation. The dominant bonding interaction between the filled b_1 on ML_2 and the LUMO of the pentadienyl cation is shown in **15a–17a** from a bottom view. The

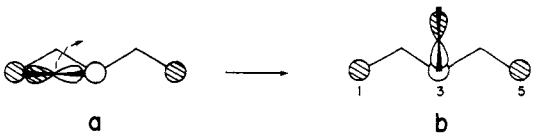

15

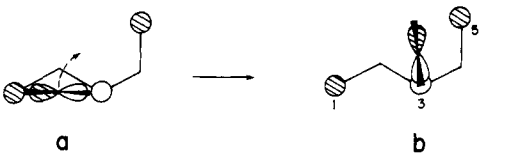

16

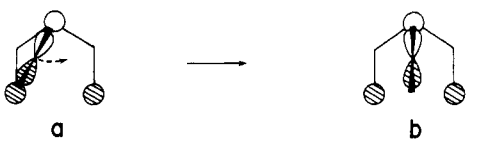

17

analogous interactions at the transition state are given by **15b–17b**. It is clear that overlap between b_1 and the pentadienyl LUMO is greatly diminished on going from the ground to transition state for **15**; the large distance between C_1 and C_5 ($\sim$4.88 Å) precludes much interaction between the p atomic orbitals on C_1 and C_5 and the shaded lobe of b_1. Therefore, there should be a substantial activation energy associated with a haptotropic rearrangement in the W isomer of η^3-pentadienyl–ML_2. The situation for the sickle isomer is slightly better. The distance between C_1 and C_5 decreases to $\sim$4.23 Å, so the overlap between the pentadienyl LUMO and b_1 in **16b** should be somewhat larger than that in **15b**. Finally, the ML_2 shift in the U isomer is clearly expected to be the most facile. The distance between C_1 and C_5 is now $\sim$2.44 Å; a sizable portion of the b_1-pentadienyl LUMO overlap is retained in **17b**. The dashed arrows in **15a–17a** indicate the direction that the ML_2 unit must migrate. The haptotropic rearrangements in the W (**12**) and U (**14**) isomers are narcissistic reactions.[12] The reactant and product are related by a fixed mirror plane and, therefore, the transition state will be one where the ML_2 unit lies on a mirror plane which bisects the pentadienyl ligand.[13] This

(11) (a) Hoffmann, R. *Angew. Chem.* **1982**, *94*, 725; *Angew. Chem., Int. Ed. Engl.* **1982**, *21*, 711. (b) Albright, T. A. *Tetrahedron* **1982**, *38*, 1339. (c) Albright, T. A.; Burdett, J. K.; Whangbo, M.-H. "Orbital Interactions in Chemistry"; Wiley: New York, 1985.

(12) Salem, L.; Durup, J.; Bergeron, G.; Cazes, D.; Chapuisat, X.; Kagan, H. *J. Am. Chem. Soc.* **1979**, *92*, 4472.

(13) A less likely possibility is that this geometry is an intermediate and two equivalent transition states lie on either side of it.

is not the case for the sickle isomer. There is no reason why the two end points in this reaction, **13a** and **13b**, should lie at equivalent energies, but in the context of our topological model, they should be very close since the p atomic coefficients at C_1 and C_5 are equal. Notice that in each case, the ML_2 unit must rotate with respect to the polyene so that the unshaded lobe of b_1 maintains overlap with the p orbital at C_3. Alternative conformations, such as those shown in **18**, for the haptotropic rearrangements are not expected to be viable. In each case, the critical

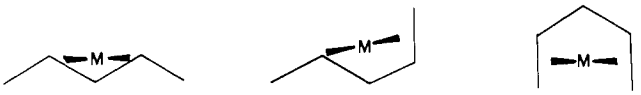

a b c

18

overlap between the b_1 HOMO of ML_2 and pentadienyl cation LUMO is totally lost. We now turn to the details of the calculations and see to what degree these predictions are supported by the actual computational results.

We shall first examine the haptotropic shift for the W isomer of η^3-pentadienyl-ML_2, **12**. To our knowledge, there is no report of such a fluxional process.[14] In terms of the computational model, we have choosen M = Pt and L = PH_3, so the complex is cationic. Additional geometrical and computational parameters for the extended Hückel calculations are supplied in the Appendix. The resultant potential energy surface is shown in Figure 2. The distance of the Pt atom to the plane of the pentadienyl fragment was initially held constant at 1.95 Å. The distance scale on the upper left side of the Figure is plotted in 0.2-Å intervals. The energy contours are in kilocalories/mole relative to the ground state, the η^3 geometry (**12**), which is indicated by a solid circle. At each point on the energy surface, the dihedral angle of the ML_2 unit relative to the pentadienyl ligand was optimized and the corresponding value was used to plot the contours. The minimum-energy reaction path is indicated by a dashed line and the transition state by a cross. The calculations point to a sizable 29.5 kcal/mol barrier that must be overcome for the haptotropic rearrangement. The binding energy of the $Pt(PH_3)_2$ unit to pentadienyl cation at the η^3 ground state is ~40 kcal/mol, whereas that at the transition state is only ~10 kcal/mol. While these numbers are not expected to be reliable in a quantitative sense at the extended Hückel level, they do point to the fact that a substantial amount of the bonding between the two fragments is lost at the transition state. A least-motion pathway which passes in a straight line between the two equivalent group states is avoided due to the high-energy region encountered underneath C_3. In other words, we find no tendency for the $Pt(PH_3)_2$ unit to attain an η^1 geometry. The evolution of the ML_2 orientation along the reaction path is shown in **19**. It follows exactly the prediction made in

19

15 by optimizing the overlap between the LUMO of the pentadienyl cation and the b_1 HOMO of $Pt(PH_3)_2$.

Let us now turn our attention to the electronic structures and exact geometries of the ground and transition states. As shown in Figure 2, at the η^3 ground state, the Pt atom is not equidistant

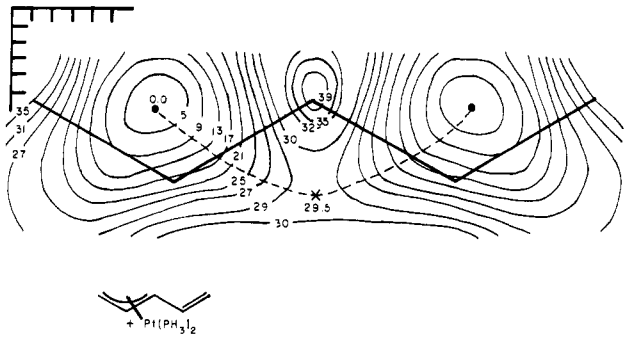

Figure 2. Potential energy surface for shifting the $Pt(PH_3)_2$ unit relative to the W-pentadienyl cation ligand. The distance scale at the upper left side of the figure is plotted in 0.2-Å intervals and the energy contours are in kilocalories/mole. The solid circles represent ground-state minima, and the transition state is indicated by a cross. The minimum energy reaction path is shown by the dashed line. The distance of the $Pt(PH_3)_2$ group to the pentadienyl plane was held constant at 1.95 Å.

to C_1 and C_3. A full optimization was carried out, varying independently the distances r_1, r_2, and h defined in **20**. The

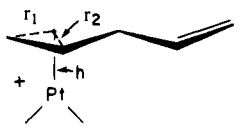

20

minimum energy was found for the set r_1 = 1.10 Å, r_2 = 0.62 Å, and h = 1.86 Å. The Pt–C_1 distance is then 2.16 Å, while Pt–C_3 = 2.30 Å. The molecular orbitals of the complex are constructed in Figure 3 at r_1 = 1.221 Å (where the Pt–C_1 and Pt–C_3 distances are equal) to examine this distortion. On the left side of the figure are three π orbitals of the pentadienyl cation. The highest two π orbitals are not important in this discussion and are not shown. At low energy, π_1 is stabilized primarily by the $1a_1$ and $3a_1$ fragment orbitals of $Pt(PH_3)_2$. There is also a very strong interaction between π_3 and b_1 to produce the 6a molecular orbital. The b_2, a_2, and $2a_1$ fragment orbitals of $Pt(PH_3)_2$ are left basically nonbonding. Finally, metal $1a_1$ and π_2 enter into a four-electron destabilizing interaction to produce the 2a and 7a molecular orbitals. Because of the lack of symmetry, π_3 mixes also into 7a to prevent it from rising too high in energy. The composition of 7a was found to be 15%(π_3) + 15%(π)2) + 70%($1a_1$). This molecular orbital is drawn from a bottom view in **21**. The net

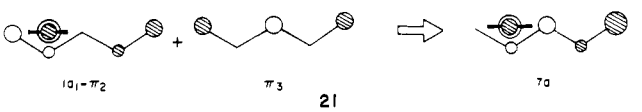

21

result is to create antibonding between C_3 and Pt, and, therefore, the ML_2 unit slips slightly toward C_1.

The transition state structure was also optimized in terms of varying x and h, as defined in **22**. The optimum values were x = 0.84 Å and h = 2.00 Å. The energy was computed to be 30.0 kcal/mol higher than the optimized ground state, **20**. There are

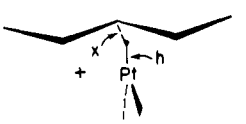

22

two electronic factors that contribute to this barrier. At the η^3 ground state, the overlap between π_3 and $Pt(PH_3)_2$ b_1 is 0.183. This is reduced to 0.072 at the transition state. Consequently, the molecular orbital corresponding to 6a in Figure 3 rises in energy. The other stabilizing interaction between the pentadienyl cation and $Pt(PH_3)_2$ occurs between π_1 and $3a_1$. The overlap actually increases slightly along the reaction path; at η^3, it is 0.346 while at the transition state it is 0.367.[15] The other electronic

(14) A preliminary communication has appeared on a 1,4-diphenyl-3-acetylpentadienyl–Pd(acac) complex; see: Sonada, A.; Mann, B. E.; Maitlis, P. M. *J. Organomet. Chem.* **1975**, *96*, C16. The haptotropic rearrangement in all likelihood proceeds via the sickle rather than W conformation, and the activation energies reported are suspiciously close to those reported for η^3-cycloheptadienyl–Pd(acac) complexes where the geometry of the pentadienyl portion is forced to be of the U type (vide infra).

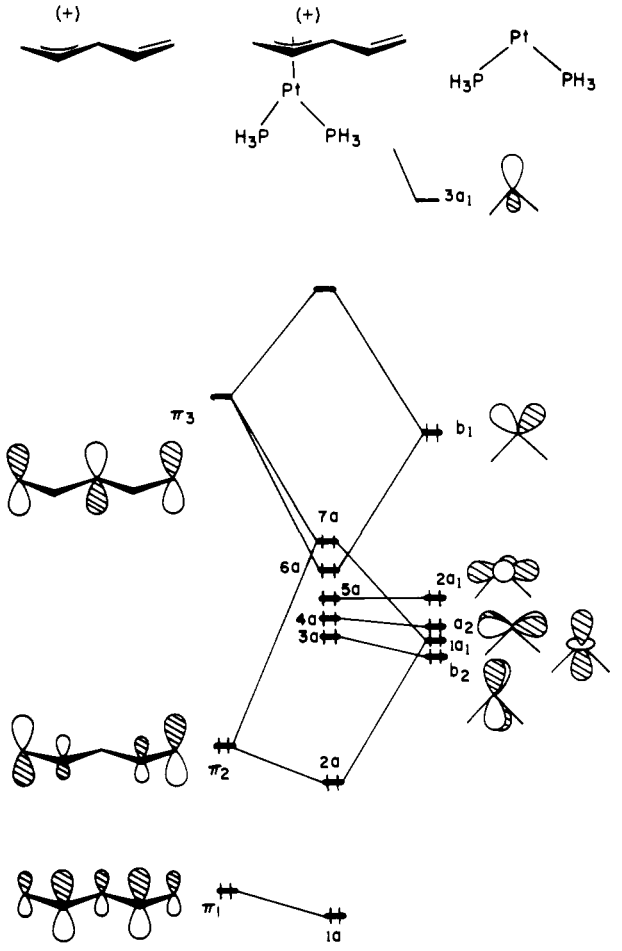

Figure 3. Orbital interaction diagram for the W isomer of pentadienyl–$Pt(PH_3)_2^+$ at the η^3 geometry.

factor which contributes to the barrier comes from the fact that at the transition state, π_2 and the ML_2 b_2 orbital are now of the same symmetry. They form bonding and antibonding combinations which are *both* filled. The antibonding combination, shown from a bottom view in **23**, is destabilized more than the bonding combination is stabilized. Diminishing this interaction should

23

render the haptotropic rearrangement more facile. An obvious way to accomplish this task is by the substitution of ligands at the metal which are stronger π acceptors than phosphines. This causes b_2 to be hybridized away from the polyene,[16] as illustrated in **24** where the π-acceptor function on each of the two ligands is symbolized by a single p atomic orbital. This hybridization

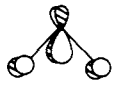

24

decreases the b_2–π_2 overlap, and, therefore, the activation energy

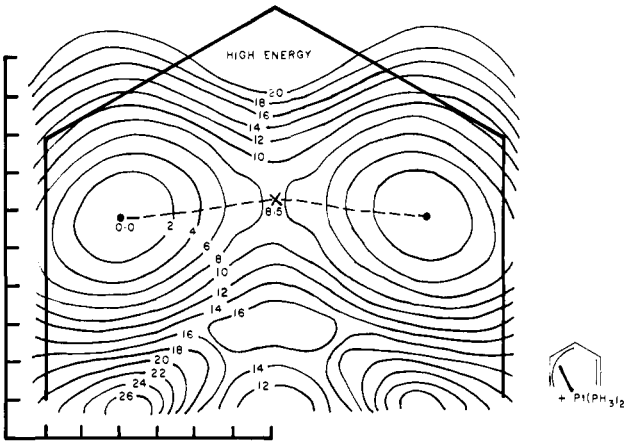

Figure 4. Potential energy surface for the U isomer of pentadienyl–Pt-$(PH_3)_2^+$. The details for the surface are the same as those given in Figure 2. The Pt–pentadienyl distance was held constant at 1.95 Å.

will be lowered. This strategy can be exploited for many of the systems that we shall discuss.

The haptotropic rearrangement of the U isomer of pentadienyl–$Pt(PH_3)_2^+$ is strikingly different. The topological analysis in **17** indicates that the rearrangement should proceed with a much lower energy than in the W isomer. The potential energy surface for shifting the $Pt(PH_3)_2$ at a constant height, 1.95 Å from the plane of the pentadienyl cation, is given in Figure 4. For each point on the surface, the orientation of the ML_2 unit with respect to the pentadienyl ligand was again optimized. An η^3 geometry was found to be the ground state. The optimum conformation of the ML_2 group along the reaction path is diagrammed in **25**.

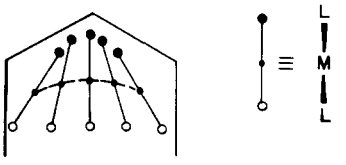

25

The computed low activation energy and orientation of ML_2 along the reaction path is in complete agreement with our simple topological analysis and that given previously by Mingos and Nurse.[4c] To further refine the barrier, we independently optimized the ground and transition states. Using the parameters defined in **26** and varying the distance of Pt to the plane of the pentadienyl ligand, h, we find the ground state to be at r_1 = 0.96 Å, r_2 = 0.42 Å, h = 1.82 Å, and α = 169°. The Pt atom is slightly closer

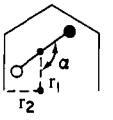

26

to C_1 than C_3 for the same reason as was presented for the W isomer. This geometry is in agreement with an early structure of η^3-cycloocta-2,4-dienyl–Pd(acac).[17] Unfortunately, the precision of the structure was not high enough to differentiate the two Pd–C distance, and it may well be the case that conformation of the eight-membered ring obscures this issue. The optimal geometry of the η^5 transition state was found to be at r_1 = 1.00 Å, r_2 = 1.22 Å, h = 1.83 Å, and α = 180°. It was computed to be 8.7 kcal/mol higher than the η^3 geometry.[18] The principal

(15) The reader may have noted from **15** that an alternative reaction path where the ML_2 unit rotates in a counterclockwise fashion and migrates in a direction toward the bottom of the structure is also possible. The ML_2 unit will, however, be much further from C_2 and C_4 at the transition state and, therefore, the overlap between π_1 and $3a_1$ becomes substantially smaller.

(16) Mingos, D. M. P. *Adv. Organomet. Chem.* **1977**, *15*, 1. There is also a high-lying empty p orbital on the ML_2 unit which can also serve to hybridize b_2 in a direction away from the polyene. Thus, a low d–p promotion energy in the metal atom will decrease the b_2–π_2 interaction.

(17) Churchill, M. R. *Inorg. Chem.* **1966**, *5*, 1608.

(18) It is interesting that the structure of 2,4-dimethylpentadienyl–Co-$(PEt_3)_2$, which is isoelectronic to the complexes studied here, is η^5 in the solid state; see: Bleeke, J. R.; Peng, W.-J. *Organometallics* **1984**, *3*, 1422. The orientation of the ML_2 unit corresponds to that proposed for the transition-state structures in the PdL_2^+ and PtL_2^+ complexes.

stabilizing overlap between metal b_1 and π_3 is only slightly reduced along the reaction path. At η^3, it is 0.191, while at the η^5 transition state it is 0.174. We are in agreement with Mingos and Nurse's analysis[4c] that a significant portion of the energy difference between the η^3 and η^5 geometries is due to the destabilizing interaction between the b_2 ML_2 fragment orbital and π_2 of the pentadienyl cation which is maximized at η^5. This is shown from a bottom view in **27**.

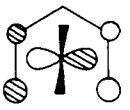

27

Mann and Maitlis have studied this rearrangement for a series of related cycloheptadienyl–PdL_2 complexes.[19] The value of $\Delta G^{\ddagger}$ found for the $Pd(PEt_3)_2^+$ case was 9.5 kcal/mol. They have also convincingly shown that the rearrangement cannot proceed via an η^1 intermediate where the Pd is bonded to C_3 (notice in Figure 4 that this corresponds to a high-energy region in the potential energy surface). Returning to **25**, at the η^3 ground state, the two auxiliary ligands are diastereotopic (being represented as open and closed circles). This is retained at the η^5 transition state; therefore, the two ligands should not exchange with each other during the course of the fluxional motion. This has been experimentally demonstrated[19] for cycloheptadienyl–Pd(acac). Since a large fraction of the barrier is derived from the increase in the destabilizing b_2–π_2 interaction, **27**, rather than loss of b_1–π_3 overlap, **17**, the activation energy should be quite sensitive to the nature of the auxiliary ligands. As outlined previously for the W isomer, substitution of π-acceptor ligands creates a smaller b_2–π_2 overlap and the barrier should decrease. The work of Mann and Maitlis[19] on the cyloheptadienyl–PdL_2 series nicely confirms this hypothesis. The values of $\Delta G^{\ddagger}$ range from 16.6 kcal/mol for L_2 = acac to ~6.8 kcal/mol for 1,5-cyclooctadiene in the order acac > ethylenediamine > PR_3 > $P(OMe)_3$ > olefin.

According to the topological analysis outlined in **15**–**17**, the activation energy for the sickle isomer should lie between that for the U and W forms. The potential energy surface is presented in Figure 5. The η^3 geometry in **9a** is found to be the global minimum (represented by the solid circle), while **9b** is a local minimum (represented by the open circle). The position of the two η^3 geometries and the transition state interconnecting them was further refined to the values given in **28**. Here *h* again is

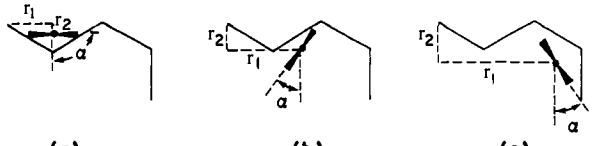

	(a)	(b)	(c)
r_1	1.14 Å	2.08 Å	3.15 Å
r_2	0.08 Å	0.66 Å	1.07 Å
α	90°	28°	30°
h	1.84 Å	1.98 Å	1.80 Å
E_{rel} (kcal/mol)	2.1	22.0	0.0

28

the distance between the Pt atom and the plane of the pentadienyl ligand. Note that the relative energies of the global and local minima have reversed themselves upon further optimization; however, they are close enough so that our extended Hückel values should not be relied upon to decide this issue. Recall that stability of the two η^3 geometries is expected to be equal by considering

(19) Mann, B. E.; Maitlis, P. M. *J. Chem. Soc., Chem. Commun.* **1976**, 1058.

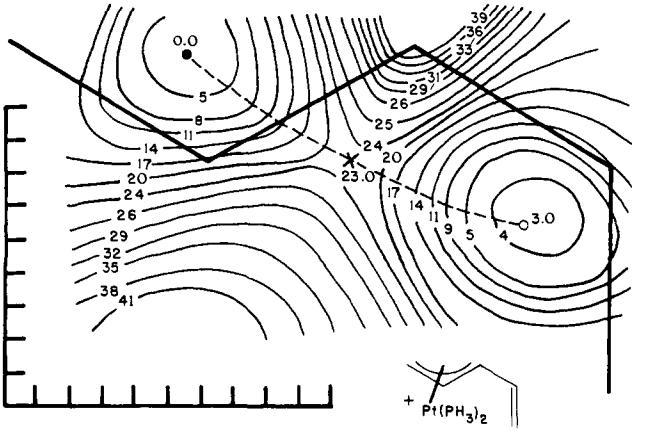

Figure 5. Potential energy surface for the sickle isomer of pentadienyl–$Pt(PH_3)_2^+$. The distance of the Pt–pentadienyl plane was held constant at 1.90 Å. Details of the surface are given in Figure 2. Here the closed circle represents the global minimum and the open circle is a local minimum.

only the metal b_1–π_3 interaction. One can see in **28** that the evolution of the ML_2 orientation along the reaction path follows the prediction made in **16**. The computed activation energy of 22 kcal/mol falls neatly between that for the U and W isomers (9 and 30 kcal/mol, respectively). We are aware of one case in the literature where an interconversion analogous to this has been reported;[20] it is shown in **29** and **30**. The $PdCl(PPh_3)$ complex exists solely as **29**, whereas the Pd(acac) compound is found to be **30**. NMR studies at room temperature for both compounds

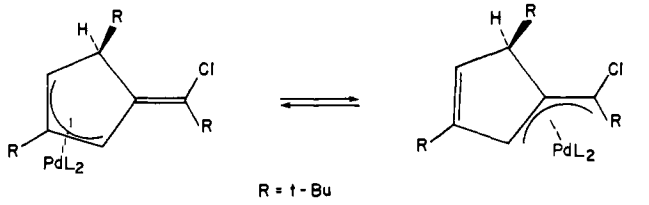

29 **30**

show no indication of an interconversion; however, the PdCl dimer is a 30:70 mixture of **29**/**30**.[20] What is perplexing is that the activation energy for the **29**–**30** interconversion in this compound was measured to be only 9.9 kcal/mol.[20a] This is not in agreement with our computations on the pentadienyl–$Pt(PH_3)_2^+$ series or the topological model presented in **15**–**17**.[21] We encourage further experimental work to establish more clearly this important point.

η^3-Benzyl- and Phenalenium–ML_2 Complexes

As outlined in the Introduction, there is good experimental evidence that the haptotropic rearrangement of 16-electron η^3-benzyl–ML_2 complexes do not proceed via η^1 intermediates.[6a,d,e] There are three conceivable alternatives for the rearrangement in **1** which has been redrawn from a bottom view in **31** and **32**. A least-motion path involves the ML_2 unit migrating over the C_6–C_7 bond along with ML_2 rotation in a clockwise sense. The proposed transition state (or intermediate) is shown in **33**. The ML_2 unit could also rotate in a counterclockwise sense along with migration inside the periphery of the benzyl ring to yield the endocyclic η^3 geometry, **34**. This may rearrange via the η^5 geometry, **35**, to the symmetry-related η^3-endocyclic structure and, finally, migration to **32** will follow the reverse of the **31**-to-**34** pathway. Finally, the exocyclic η^3 complex, **31**, could migrate directly to the η^5 structure, **35**, and back again to **32**. An important experimental[6a,b,d] feature of this reaction is that L_1 and L_2 must

(20) (a) Bailey, P. M.; Mann, B. E.; Segnitz, A.; Kaiser, K. L.; Maitlis, P. M. *J. Chem. Soc., Chem. Commun.* **1974**, 567. (b) Mann, B. E.; Bailey, P. M.; Maitlis, P. M. *J. Am. Chem. Soc.* **1975**, *97*, 1275.

(21) The barrier for the cycloheptatrienyl–PdCl dimer where the pentadienyl portion of the ligand is constrained to be in the U form has been measured[19] to be 15.1 kcal/mol which is significantly larger than that found for **29**.

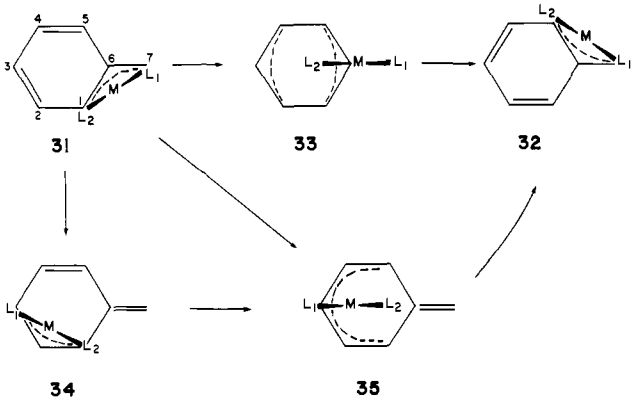

remain stereochemically distinct. In other words, L_1 and L_2 remain cis and trans, respectively, to C_7 on going from **31** to **32**.

Before the numerical results are presented, let us examine these paths by the topological analysis and our experience with the pentadienyl-ML_2 complexes. The most important π orbitals of the benzyl system are shown in **36**. We shall artifically partition

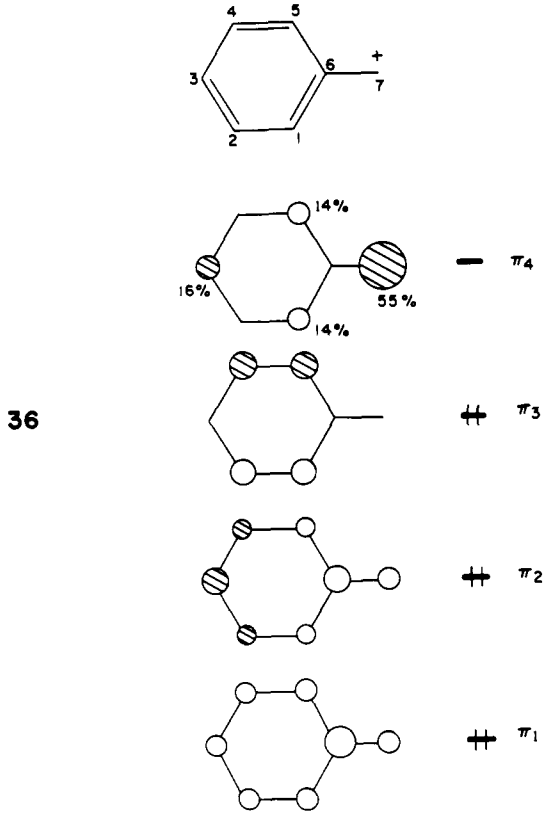

36

the complex into a benzyl cation and d^{10} ML_2 unit. The leading interaction is then between the HOMO, b_1, in ML_2 and the LUMO, π_4, in the benzyl cation. This is shown from a bottom view at the η^3 ground state in **37**. Overlap between b_1 and π_4

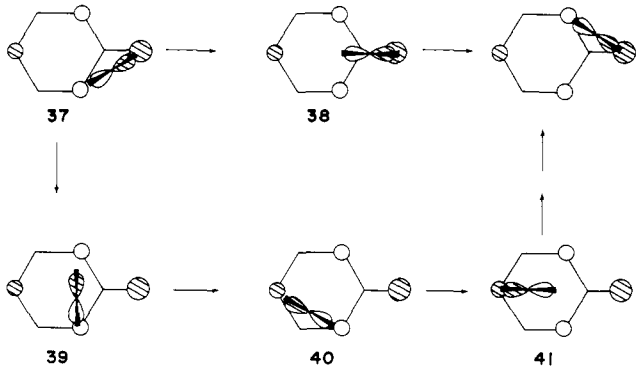

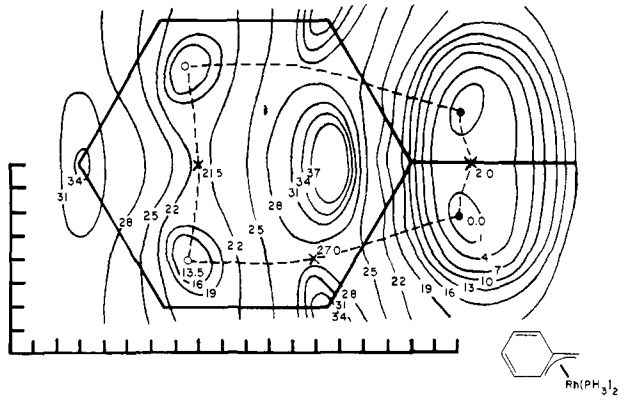

Figure 6. Potential energy surface for benzyl-$Rh(PH_3)_2$. The distance between Rh and the benzyl ligand was fixed at 2.03 Å. Details concerning the surface are given in Figures 2 and 5.

is maintained in the least-motion pathway; see **38**. While some overlap between the unshaded lobe of b_1 and the p atomic orbital at C_1 is lost, this is compensated by a gain in overlap to the atomic orbital at C_5. Thus, the direct path from **31** to **32** via **33** is expected to be facile. Rotation of the ML_2 unit in the opposite sense and migration into the interior of the benzyl ring conserves overlap between the unshaded lobe of metal b_1 and the p atomic orbital at C_1, as shown in **39** and **40**. Topologically, this is similar to the situation encountered for the shift in the sickle form of pentadienyl-ML_2 (see **16**). There are, however, two important differences. First of all, one can see from **39** that antibonding is introduced between the shaded lobe of b_1 and the p atomic orbital at C_5. Second, the three atomic coefficients in the LUMO (π_3) of the pentadienyl cation are roughly equal. Thus, approximately one-half of the overlap between b_1 and π_3 is lost at the transition state for the pentadienyl complex. In the benzyl system, the coefficients at C_7, C_1, and C_3 are not equal. The percentage contribution of the p orbitals for π_4 are given in **36**. π_4 is concentrated on C_7 with much smaller coefficients at C_1, C_3, and C_5. Since overlap between the shaded lobe of b_1 at the p atomic orbital at C_7 is lost on going to **39**, the overlap between b_1 and π_4 is greatly diminished for this reason as well. The activation energy for the **31**-to-**34** rearrangement, therefore, should be larger than that found in the sickle isomer of pentadienyl-ML_2. It is certainly predicted to be of higher energy than the least-motion path via **33**. The smaller atomic coefficients at C_1 and C_3 in the benzyl ligand should make the endocyclic η^3 geometry (**34**) less stable than the exocyclic η^3 one (**31**); i.e., compare **37** with **40**. Finally, the rearrangement of the endocyclic η^3 structure to the η^5 species (**35**) is topologically identical with the rearrangement in the U form of pentadienyl-ML_2; compare **40** and **41** with **17**. Consequently a similar activation energy is anticipated for the two processes.

Computations on this system were carried out for benzyl-$Rh(PH_3)_2$. The potential energy surface for shifting $Rh(PH_3)_2$ relative to the benzylic unit is shown in Figure 6. The distance of the Rh to the plane of the cycle was initially held constant at 2.03 Å. Global minima are found at the two equivalent, exocyclic η^3 positions (indicated by the solid circles). In the optimized structure, we find the distances of Rh to C_1, C_6, and C_7 to be 2.45, 2.25, and 2.20 Å, respectively. These are in good agreement with the structure[6d] of $[\eta^3\text{-}CH_2C_6(CH_3)_5]Rh[P(O\text{-}i\text{-}C_3H_7)_3]_2$ where the corresponding distances are 2.45, 2.25, and 2.13 Å. The structures of all benzyl-ML_2 complexes[6c,d,g] and what we calculate for the ground-state geometry in benzyl-$Rh(PH_3)_2$ are significantly distorted from the structures of the related π-allyl-ML_2 compounds.[22] First, the metal-C_7 distance is much shorter than that to C_1. In other words (see Figure 6), the projection of the metal

(22) For an early review, see: Clark, H. L. *J. Organomet. Chem.* **1974**, *80*, 155. A full listing may be found in: Albright, T. A.; Hoffmann, R.; Tse, T.-C.; D'Ottavio, T. *J. Am. Chem. Soc.* **1979**, *101*, 3812.

atom onto the plane of the cycle does not lie on the bisector of the C_1–C_6–C_7 angle. Notice that π_4 in **36** is much more concentrated at C_7 than it is at C_1. Therefore, the overlap between b_1 and π_4 is increased when the ML_2 unit is shifted toward C_7. There are further secondary mixings, particularly between the filled $2a_1$ orbital on ML_2 (see Figure 1) and empty π_4, which also favor this distortion. Second, the projection of the metal onto the plane of the cycle lies well inside the triangle defined by C_1, C_6, and C_7. The reason behind this is a very soft potential for distortion along the least-motion reaction path which interconverts the two ground states. We find the transition state to lie only 2.0 kcal/mol above the ground state. The orientation of the $Rh(PH_3)_2$ unit is exactly that predicted by **38**, namely the plane of the ML_2 fragment is parallel to the C_6–C_7 axis. The overlap between b_1 and π_4 actually increases on going from the optimized ground to transition state (0.272 vs. 0.296, respectively). A barrier results from the repulsion between the filled π_3 benzyl orbital and b_2 orbital on ML_2. The occupied antibonding combination is shown from a bottom view in **42**. To our knowledge, a static η^3

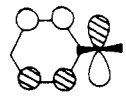

42

structure has never been observed by NMR studies for 16-electron benzyl–ML_2 complexes.[6] An upper limit of ~6.4 kcal/mol has been estimated for trityl–Pt(acac) with an even lower barrier for the Pd complex.[6b]

Let us now turn our attention to the alternative pathway which connects the exocyclic η^3 structure, **31**, to the endocyclic η^3, **34**, and η^5, **35**, geometries. Local minima, given by the open circles, in Figure 6 were found for the endocyclic η^3 isomers. They lie 13.5 kcal/mol above the ground state. The reason for this was outlined previously in terms of our topological model. Since the coefficients at C_1 and C_3 are much smaller than that at C_7 in π_4, the overlap between π_4 and the ML_2 b_1 orbital is substantially smaller at the endocyclic η^3 structure. The optimum value of the π_4–b_1 overlap was found to be 0.121, whereas it is 0.272 at the exocyclic η^3 geometry. Interconversion between the two equivalent endocyclic η^3 geometries proceeds via an η^5 transition state and requires 8.0 kcal/mol. This rearrangement is strictly analogous to that given for the U form of pentadienyl–ML_2. The optimal orientation of the ML_2 unit corresponds to that given in **41** which again maximizes the π_4–b_1 interaction. The crucial feature of the surface concerns the migration of ML_2 between the endo and exocyclic η^3 positions. Recall from the topogotical analysis given for **39** that while the basic nodal structure in π_4 is similar to that in the sickle form of pentadienyl–ML_2, the activation energy for this rearrangement should be considerably higher. The transition state for benzyl–$Rh(PH_3)_2$ lies 27.0 kcal/mol above the ground state. In fact, this is approximately the computed binding energy between the benzyl and $Rh(PH_3)_2$ fragments. The conformation of the ML_2 unit along this reaction channel is also interesting. Its evolution is depicted in **43**. The antibonding introduced

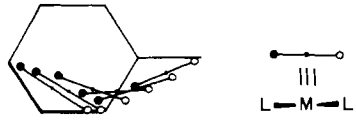

43

between the shaded lobe of b_1 and the p orbital at C_5 is large enough in **39** to prohibit the ML_2 unit from rotating in a clockwise sense. It instead undergoes a lateral sliding motion as it crosses the C_1–C_6 bond.

In summary, the minimum energy reaction path that we compute for the **31**- to **32**-rearrangement is the least-motion one via **33**. The alternative paths from **31** to **34** or **31** to **35** have all the earmarks of a symmetry-forbidden sigmatropic rearrangement.[23]

A number of 16-electron phenalenium–ML_2 complexes exist[9] which potentially can undergo the haptotropic rearrangement shown in **44**. There are a number of interesting parallels here

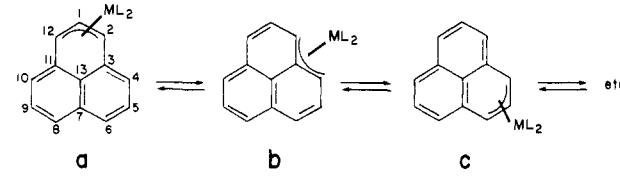

44

to the pentadienyl and benzyl systems which we shall briefly explore. One can partition the molecule into a d^{10}-ML_2 unit interacting with a phenalenium cation. The dominant interaction will be between the filled b_1 orbital of ML_2 and the LUMO of the phenalenium cation. This is shown for the ground-state geometry, **44a**,[9b] in **45a**. Migration to the alternative η^3 geometry,

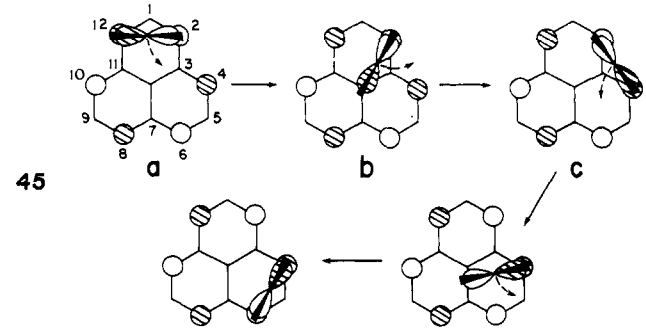

45

44b, requires passage through a geometry akin to that shown in **45b**. Notice that this rearrangement is again topologically similar to that for the sickle isomer of pentadienyl–ML_2. Overlap between the unshaded lobe of b_1 and the p atomic orbital at C_2 is retained in **45b**; while not much overlap exists between the shaded lobe of b_1 and the p orbitals at C_4 and C_{12}. Unlike the exo-to-endocyclic η^3 migration in benzyl–ML_2, antibonding between the shaded lobe of b_1 and the p orbital at C_{10} is not expected to be significant (compare **39** with **45b**) since the distance between the metal and C_{10} in **45b** is much longer than the analogous metal–C_5 distance in the benzyl system. The coefficients of the p atomic orbitals at C_2, C_4, C_6, C_8, C_{10}, and C_{12} in the phenalenium cation LUMO are identical by symmetry. Therefore, the overlap between the two fragment orbitals in **45a** is identical with that in **45c**. One then expects that there should be little energy difference between the two η^3 isomers **44a** and **44b**. A structure close to that shown in **45b** will serve as the transition state for this rearrangement, and the corresponding activation energy is expected to be similar to that in the sickle isomer of pentadienyl–ML_2 complexes.

Computations on phenalenium–$Pt(PH_3)_2^+$ fully confirmed these predictions. We shall only cover the most important features here. The optimized ground-state structure, **44a**, is close to that found[9b] for 6-ethoxyphenalenium–$Pt(PPh_3)_2^+$. The Pt–C_1, Pt–C_2(C_{12}) distances were found to be 1.99 and 2.31 Å, respectively, compared to 2.17 and 2.27 Å (averaged) in the experimental structure. The preferred orientation of the ML_2 unit (shown in **45a**) matches that in the X-ray structure. A barrier of 20.0 kcal/mol is found for the transition state which connects **44a** with **44b**, and the orientation of the ML_2 unit is that given in **45b**. Notice that the barrier here is quite close to the computed one in the sickle isomer of pentadienyl–$Pt(PH_3)_2^+$ (22 kcal/mol). This is consistent with NMR investigations on phenalenium–ML_2 complexes which, as mentioned in the Introduction, have shown that $\Delta G^{\ddagger}$ ~18 kcal/mol.[9a] The alternative η^3 isomer, **44b**, was found to be only 3.8 kcal/mol higher in energy than the ground state.

(23) Woodward, R. B.; Hoffmann, R. "The Conservation of Orbital Symmetry"; Verlag Chemie: Weinheim, 1984; pp 114–140. Fleming, I. "Frontier Orbitals and Organic Chemical Reactions"; Wiley: New York, 1976; pp 98–103. Nguyen. T. A. "Les regles de Woodward-Hoffmann". German translation; Verlag Chemie; Weinheim, 1972; pp 59–112.

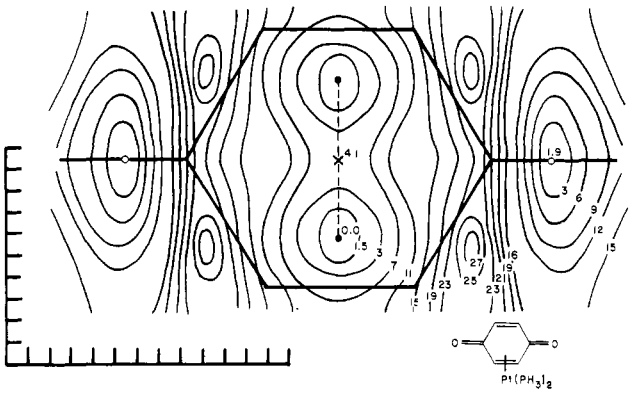

Figure 7. Potential energy surface for quinone–$Pt(PH_3)_2$. The distance between Pt and the quinone ligand was held constant at 1.90 Å. Other computational details are given in Figures 2 and 5.

η^2-Polyene-ML_2 Complexes

The previous examples were of the 16-electron η^3 type; we now turn our attention to complexes which have a 16-electron η^2 coordination for the ground-state structure. d^{10}-Quinone-ML_2 complexes have been known since the early 1960s.[24] Both η^2, **46**,[25] and η^4, **47**,[26] isomers have been structurally categorized. NMR

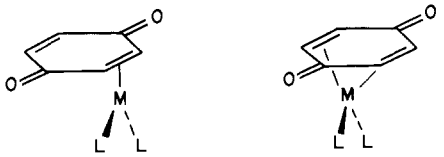

46 **47**

investigations at low temperature on η^2 complexes[25a,26a,27] have shown a very facile dynamic behavior which equivalences the two halves of the quinone ligand. In fact, the ^{13}C rate-limiting spectrum has been achieved for only one complex, 2,6-dimethylquinone–$Pt(C_2H_4)[P(C_6H_{11})_3]$,[26a] at −90 °C. Thus, it is reasonable to expect that the energy difference between **46** and **47** is very small, and if the ground-state geometry is η^2, then the η^4 structure will serve as the transition state for this haptotropic rearrangement.

The dominant interaction in this complex, between the filled b_1 orbital in the d^{10} ML_2 fragment and the LUMO of quinone, is displayed from a bottom view at the η^2 geometry in **48**. A

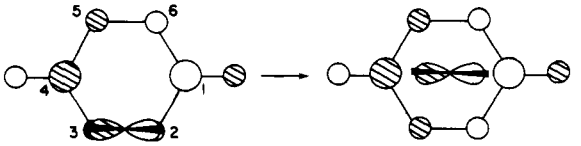

48 **49**

least-motion slippage of the ML_2 unit to the η^4 geometry, **49**, where no rotation of ML_2 occurs conserves overlap between these two fragment orbitals. In fact, the p orbital coefficients at C_1 and C_4 are larger than those of C_2 and C_3; there is a larger overlap between the two fragment orbitals in **49** than there is in **48**. Extended Hückel calculations on quinone–$Pt(PH_3)_2$ at η^2 and η^4 gave overlap values of 0.142 and 0.192 for **48** and **49**, respectively. Thus, barring any other electronic effects, the η^4 geometry should be more stable than η^2.

The potential energy surface for quinone–$Pt(PH_3)_2$ is given in Figure 7. The Pt–quinone plane distance was held constant at 1.90 Å. The two equivalent global minima, represented by the solid circles, are shifted significantly away from η^2 toward the η^4 position. The η^4 geometry at this computational level does serve as the transition state. Further geometrical optimizations were carried out by varying the distance between the projection of the Pt atom onto the plane of the quinone ligand, *h*, and the distance between the projection and bisector of the C–C bond, *r*, as defined in **50**. The global minimum was found to be at r = 0.39 Å and

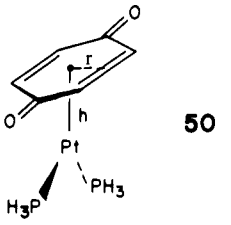

50

h = 1.88 Å. The η^4 transition state with r = 1.221 Å and h = 1.86 Å lies 3.9 kcal/mol above the ground state. The reason why the η^4 geometry is less stable than the global optimum lies in the fact that at η^4-maximum overlap occurs between the filled b_2 orbital of ML_2 (see Figure 1) and the HOMO of the quinone ligand, **51**. This four-electron two-orbital repulsion was also the

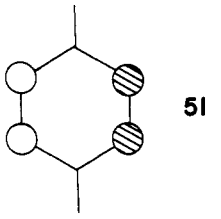

51

essence of the barrier in the U isomer of η^3-pentadienyl–ML_2 and benzyl–ML_2. The destabilization at the η^4-quinone–ML_2 geometry can be ameliorated in a way precisely analogous to that presented in the previous sections. Substitution of electron-withdrawing ligands for the phosphines causes the b_2 orbital to become hybridized away from the quinone (see **24**). Therefore, the overlap between b_2 and **51** is minimized.[28] The quinone complexes which have been shown to possess an η^4 structure as the ground state[26] have either a 1,5-cyclooctadiene or another quinone as auxiliary ligands. In both cases, there is a low-lying LUMO of the appropriate symmetry to interact with the b_2 orbital.

Returning to the potential energy surface in Figure 7, notice that two equivalent minima are found where $Pt(PH_3)_2$ is coordinated to the carbonyl groups of the quinone in an η^2 fashion. Somewhat surprisingly, they are found to lie only 1.9 kcal/mol above the global minima. We are not aware of any isolated quinone–ML_2 complex which has structure. However, a number of examples do exist in the literature where a d^{10} ML_2 unit is coordinated in an η^2 fashion to an aldehyde or ketone.[29] Furthermore, ab initio calculations[30] on ethylene and formaldehyde–$Ni(PH_3)_2$ have shown that the ligand-to-$Ni(PH_3)_2$ binding energy in the latter compound is 12 kcal/mol greater than that in the former. Therefore, the existence of local minima for this geometry is not unwarranted. The reader can easily verify by inspection that all overlap between the metal b_2 orbital and quinone LUMO in **48** (or **49**) is lost upon migration of ML_2 to the carbonyl group of the quinone. The reaction is symmetry-

(24) Schraefer, G. N.; Thyrett, H. *J. Am. Chem. Soc.* **1960**, *82*, 6420; *Z. Naturforsch., B* **1961**, *16B*, 353.
(25) (a) Chetcuti, M. J.; Herbert, J. A.; Howard, J. A. K.; Pfeffer, M.; Spencer, J. L.; Stone, F. G. A.; Woodward, P. *J. Chem. Soc., Dalton Trans.* **1981**, 284. (b) Vagg, R. S. *Acta Crystallogr., Sect. B* **1977**, *33B*, 3708.
(26) (a) Chetcuti, M. J.; Howard, J. A. K.; Pfeffer, M.; Spencer, J. L.; Stone, F. G. A. *J. Chem. Soc., Dalton Trans.* **1981**, 276. (b) Glick, M. D.; Dahl, L. F. *J. Organomet. Chem.* **1965**, *3*, 200. (c) Aleksandrov, G. G.; Struchkov, Y. T. *Zh. Strukt. Khim.* **1973**, *14*, 1067.
(27) Ceini, S.; Ugo, R.; LaMonica, G. *J. Chem. Soc. A* **1971**, 416.
(28) Rotation of the ML_2 unit by 90° with respect to the quinone ligand will also cause overlap between b_2 and **49** to vanish. However, the stabilizing interaction between b_1 and the LUMO of the quinone also vanishes. A detailed discussion of the conformational preferences in these complexes may be found in ref 4b.
(29) (a) Countryman, R.; Penfold, B. R. *J. Cryst. Mol. Struct.* **1972**, *2*, 281. (b) Tsou, T. T.; Huffman, J. C.; Kochi, J. K. *Inorg. Chem.* **1979**, *18*, 2311. (c) Kaiser, J.; Sieler, J.; Walther, D.; Dinjus, E.; Golic, L. *Acta Crystallogr., Sect. B* **1982**, *B38*, 1584.
(30) Sakaki, S.; Kitaura, K.; Morokuma, K.; Ohkubo, K. *Inorg. Chem.* **1983**, *22*, 104.

forbidden. The corresponding activation energy is 24 kcal/mol which is essentially the binding energy between the quinone and $Pt(PH_3)_2$ fragments.

There are a number of structural perturbations within the ligand that can be considered for this type of rearrangement. The LUMO of *p*-quinodimethane, **52a**, is topologically identical with that for the quinone ligand; compare **52b** with **49**. Replacement of the

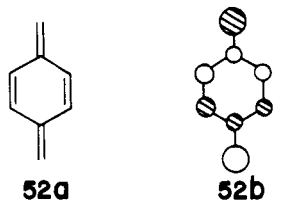

52a **52b**

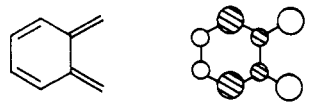

53a **53b**

two electronegative oxygen atoms with methylene groups does cause a redistribution of the density in the LUMO. As shown in **52b**, the p atomic orbital coefficients at C_1 and C_4 become much smaller. Consequently, the overlap between the ML_2 b_1 orbital and **52b** should be smaller at the η^4 geometry, compared to the quinone system, and the associated barrier should be larger. The *o*-quinodimethane ligand, **53a**, presents an interesting variation. The LUMO is shown in **53b**. The coefficients are rather evenly balanced, so that a d^{10} ML_2 fragment should bond to either of the two equivalent exocyclic η^2 or the two endocyclic η^2 positions. Because of the nodal structure in **53b**, rearrangement between one endocyclic η^2 position to the other by a least-motion path (where the ML_2 group does not rotate with respect to the quinodimethane ligand) should be facile. An identical situation occurs for interconversion between the exocyclic η^2 positions. But like the quinone and *p*-diquinodimethane–ML_2 cases, the haptotropic rearrangement from an endo-to-exocyclic η^2 geometry will not be favorable. All overlap between the b_1 ML_2 orbital and **53b** is lost along any reaction pathway. Unfortunately, no ML_2 complexes of a quinodimethane appear to have been prepared which could be used to test these predictions.

Both endocyclic η^2, **54**, and exocyclic η^2, **55**, d^{10}-ML_2 complexes of fulvenes are known.[31] There is also one example of an η^4 complex, **56**, where the two auxiliary ligands are a 1,5-cyclooctadiene group.[32] The LUMO of fulvene is shown in **57**. Again,

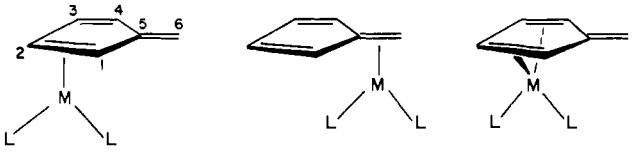

54 **55** **56**

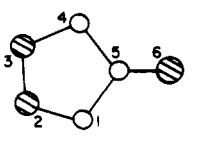

57

the topology of **57** bears a marked resemblance to that in the quinone and *p*-quinodimethane cases. Overlap is conserved for the rearrangement from one endocyclic η^2 position, **54**, to the other by way of the η^4 geometry, **56**. Shifting the ML_2 unit from the endocyclic η^2 to exocyclic η^2 position is symmetry-forbidden. Computations on fulvene–$Pt(PH_3)_2$ were carried out to check these predictions. We shall not present the potential energy surface; it is very similar to the quinone–$Pt(PH_3)_2$ system in Figure 7. Minima were found for the exo and endocyclic η^2 geometries, with the former more stable by 10.4 kcal/mol. The interconversion between the two endocyclic η^2 isomers was calculated to require 9.7 kcal/mol. The energy difference between endocyclic η^2 and η^4 structures in fulvene–$Pt(PH_3)_2$ is, therefore, somewhat larger than that in quinone–$Pt(PH_3)_2$. This is due to the smaller p atomic orbital coefficient at C_5 in the LUMO of fulvene compared to quinone. Furthermore, the HOMO of fulvene, which is topologically analogous to **51** in quinone, lies higher in energy and consequently destabilizes the ML_2 b_2 orbital more at η^4. The ground-state η^4 structure for fulvene–Pt(1,5-cyclooctadiene)[32] is consistent with this analysis since the auxiliary ligand is a strong π acceptor, and as we have pointed out previously, this will rehydridize the b_2 orbital away from the fulvene. Unfortunately, there is no experimental information on the barrier for an endocyclic η^2 $Pt(PR_3)_2$ complex. There is much greater assymmetry in the Pd–C_5, Pd–C_6 bond lengths for exocyclic η^2-1,2,3,4-tetramethylfulvene–$Pd(PMe_3)_2$[31b] (2.186 (2) vs. 2.108 (2) Å, respectively) than what we calculate for the global minimum in fulvene–$Pt(PH_3)_2$. We computed the Pt–C_5 and Pt–C_6 distances to be 2.10 and 2.09 Å, respectively. The η^2-endocyclic 6,6-diphenylfulvene–$Pt(PPh_3)_2$ Pt–C_1 and Pt–C_2 distances were found[31a] to be 2.24 (2) and 2.15 (2) Å, respectively. In our optimized structure, these distances were 2.17 and 2.09 Å, respectively. The structure of η^4-6,6-diphenylfulvene–Ni–(1,5-cyclooctadiene) also is slipped from an idealized η^4 geometry.[32] The Ni–C_1(C_4) and Ni–C_2(C_3) distances were 2.20 (1) and 2.07 (1) Å, respectively. Our optimized values for the η^4 transition state of 2.54 and 2.31 Å, respectively, show the same asymmetry. An electronic rationale for these unequal metal–carbon distances has been given elsewhere.[33]

Ring Whizzing

Migration of an ML_2 unit inside the periphery of a fully conjugated, cyclic polyene posses a special problem for the topological model that we have presented. All π orbitals of a cyclic polyene come as degenerate pairs, except for the lowest level (or the highest level in the case of even-membered cycles). In any realistic example, the interaction with the b_1 ML_2 fragment orbital will be derived from one member of the degenerate pair. In general, this will be sensitive to the exact geometry; however, one member of the degenerate set can be chosen so that some overlap with the b_1 fragment orbital is possible through the entire reaction path. Some typical examples will be presented in this section to illustrate the pattern that emerges.

As mentioned in the Introduction, ring whizzing in d^{10} cyclopropenium–$M(PPh_3)_2^+$ compounds is extraordinarily facile.[4a] The rearrangement in **58**, from an η^2 geometry to another, can be analyzed as shown in **59** where one component of the empty e″ interacts with the filled ML_2 b_1 orbital. Overlap in **59a** and **59b**

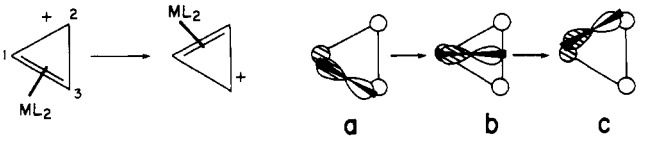

58 **59**

is retained provided that the ML_2 unit rotates in a counterclockwise sense as it moves inside the cyclopropenium ring. Furthermore, since C_2 and C_3 are directly connected, overlap between the p atomic orbitals at these carbons and the unshaded lobe of the b_1 orbital is expected to be sizable at **59b**. We have previously carried

(31) (a) Christofides, A.; Howard, J. A. K.; Spencer, J. L.; Stone, F. G. A. *J. Organomet. Chem.* **1982**, *232*, 279. (b) Werner, H.; Crisp, G. T.; Jolly, P. W.; Krause, H.-J.; Krüger, C. *Organometallics* **1983**, *2*, 1369. (c) Altman, J.; Wilkinson, G. *J. Chem. soc.* **1964**, 5654.

(32) Edelmann, F.; Lubke, B.; Behrens, U. *Chem. Ber.* **1982**, *115*, 1325.

(33) Silvestre, J. Ph.D. Dissertation, University of Houston, 1983.

out calculations on the haptotropic rearrangement in **58**.[4a] An η^2 structure was found to be the ground state, and the transition state lies only 2.9 kcal/mol above it, with a geometry indicated by **59b**. Four structures of $(Ph_3C_3)M(PPh_3)_2^+X^-$ where M = Ni, Pd, and Pt and $X^- = ClO_4^-$ and PF_6^- show a progressive movement of the ML_2 unit over the face of the cyclopropenium ring.[4a] These structures effectively chart this haptotropic rearrangement. The experimental results are totally consistent with the previous calculations and the model we have presented here.

A number of d^{10} cyclobutadiene–NiL_2 complexes have been prepared by Hoberg and co-workers.[34] There is some question in our minds whether they are η^2 and fluxional or, as proposed on the basis of ^{13}C NMR at room temperature, η^4. The leading interaction is displayed in **60** and **61**, respectively. It is clear that

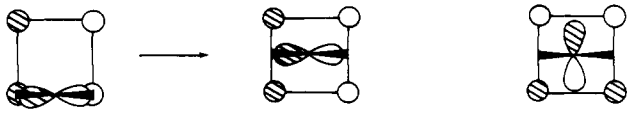

60 **61** **62**

there will not be much of an energy difference between the η^2 and η^4 structures. Just as in the quinone and fulvene systems, the filled b_2 ML_2 orbital and the HOMO of cyclobutadiene (one number of the e_g set) maximize their repulsion at η^4. The antibonding combination is displayed in **62**. It is this interaction which has been predicted[4b] to cause the cyclobutadiene ligand to adopt a rectangular geometry. For the conformation shown in **62**, the two C–C bonds which are eclipsed by the M–L bonds lengthen while the other two C–C bonds contract. Rotating the ML_2 unit by 45° causes the cyclobutadiene ligand to adopt a butterfly geometry. The two carbon atoms which are staggered by ML_2 move out of the plane of the other two carbons in a direction away from the metal. Our calculations on cyclobutadiene–$Ni(PH_3)_2$ gave an η^2 structure to be the ground state. The η^4 isomer where the Ni–P bonds eclipse two C–C bonds is a local intermediate, 2.3 kcal/mol higher in energy than η^2. There is effectively free rotation at the η^4 geometry since the alternative conformation lies only 0.1 kcal/mol higher in energy. Most importantly, it requires an activation energy of only 2.6 kcal/mol to convert the η^2 ground state to the η^4 structure. The reaction pathway is exactly that predicted from **60** and **61**. The energy differences here are certainly small enough so that computations at a higher level are warranted to make an accurate assessment.[35] Our extended Hückel calculations point to a very facile random-exchange mechanism for fluxionality in this compound.

As indicated in the Introduction, a number of substituted benzene–ML_2 complexes exist[8] where M = Ni, Pt, and L can be a variety of neutral, two-electron-donor ligands. Two structures of this type have been reported in the literature;[8d,36] both are η^2 complexes. A barrier of 11 kcal/mol has been estimated for ring whizzing in hexakis(trifluoromethyl)benzene–$Pt(PEt_3)_2$[8a] and an η^2–η^1–η^2 process has been suggested as a likely exchange mechanism.[8c] A lower barrier was found for the analogous Ni complex. Our topological analysis is shown in **63** and **64**. At the η^2 ground state, **63**, the dominant interaction occurs between the LUMO of benzene and the filled b_1 fragment orbital on ML_2.[37] The

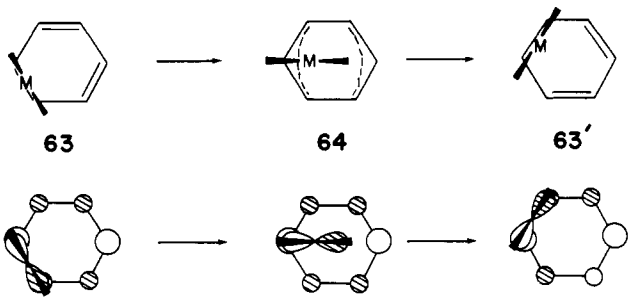

63 **64** **63′**

predicted transition state for this rearrangement is illustrated by **64**. Overlap between the two fragment orbitals is conserved only if the ML_2 unit rotates in a counterclockwise sense as it migrates. This is also the prediction obtained from Mingos' method.[3f]

Extended Hückel calculations on the η^2 structure for benzene–$Ni(CO)_2$ yielded no binding energy between the benzene and $Ni(CO)_2$ fragments. The attractive interaction between the benzene LUMO and b_1 is not strong enough to compensate for repulsions between the filled benzene π levels and filled ML_2 orbtials (primarily the interactions between $1a_1$ and a_2 of ML_2, see Figure 1, and the HOMO π set on benzene). All catergorized 16-electron arene–ML_2 complexes[8,36] in fact contain strong electron-withdrawing groups substituted on the benzene ring, the most common ligand being hexakis(trifluoromethyl)benzene. This lowers the energy of the arene π and π^* levels which in turn increases the binding energy between the two fragments. For computational efficiency, we simulated the effect of trifluoromethyl substituents by decreasing the s and p H_{ii}'s on the carbon atoms of the benzene ring by 2.5 eV. The binding energy between benzene and $Ni(CO)_2$ at the η^2 ground state is then computed to be 18 kcal/mol. The geometry of the η^3 transition state was carefully optimized by independent variation of the distance between the projection of the Ni atom onto the plane of the benzene ring, h, the projection and C_2 carbon distance, r, and the dihedral angle between C_1, C_2, and C_3 and C_4, C_5, and C_6 planes, α, in conformations **65** and **66**. Optimum values of r = 0.43 Å, h =

65 **66**

1.88 Å, and α = 10° were found for **65** which lies 9.2 kcal/mol above the η^2 ground state. Recall from **64** that this is predicted to correspond to the transition-state conformation. Suprisingly, geometry **66** with r = 0.48 Å, h = 1.88 Å, and α = 13° lies at a lower energy than **65**. It was found to be 5.9 kcal/mol above the η^2 ground state. In other words, **66** and *not* **65** is the transition state for this haptotropic rearrangement. The evolution of the ML_2 orientation along the minimum energy reaction path from one η^2 ground state to the transition state is shown in **67**.

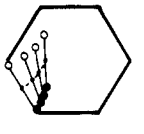

67

The rationale for why our topological model fails in this instance is interesting and has a direct parallel in organic chemistry. A $Ni(CO)_2$ group is isolobal to CH_2;[38] therefore, η^2-benzene–Ni-

(34) (a) Hoberg, H.; Fröhlich, C. *J. Organomet. Chem.* **1981**, *209*, C69. (b) Hoberg, H.; Richter, W.; Fröhlich, C. *Ibid.* **1981**, *213*, C49. (c) Hoberg, H.; Richter, W. *Ibid.* **1980**, *195*, 347, 355. (d) Hoberg, H.; Fröhlich, C. *Angew. Chem.* **1980**, *92*, 131. (e) Griebsch, U.; Hoberg, H. *Ibid.* **1978**, *90*, 1014.

(35) The very facile cycloaddition of tetramethylcyclobutadiene–Ni(bpy) with olefins (see ref 34e) is perhaps more consistent with an η^2 ground state. Complexes with two electrons less apparently do not react in this manner and have been established to be η^4 with a square cyclobutadiene structure; see: Hemmer, R.; Brune, H. A.; Thewalt, U. *Z. Naturforsch., B* **1981**, *36B*, 78. Schmitt, H.-J.; Weidenhammer, K.; Ziegler, M. L. *Chem. Ber.* **1976**, *109*, 2558. Fenske-Hall computations have been carried out for the η^4 isomer; see: Chinn, J. W., Jr.; Hall, M. B. *J. Am. Chem. Soc.* **1983**, *105*, 4930. Bursten, B. E.; Fenske, R. F. *Inorg. Chem.* **1979**, *18*, 1760.

(36) Cobbledick, R. E.; Einstein, F. W. B. *Acta Crystallogr., Sect. B* **1978**, *B34*, 1849.

(37) Notice that for both the cyclopropenium and benzene–ML_2 cases, the member of the degenerate set on the polyene was chosen to be the one which can overlap continuously along the reaction path with the ML_2 b_1 orbital. In both cases if the η^2 ground state possess C_s symmetry, b_1 actually overlaps with the alternative member of the degenerate set. However, at small excursions from the η^2, C_s structure, the overlap shown in **59a** and **63** is sizable.

$(CO)_2$ is isolobal to norcaradiene, **68**. The [1,5]-sigmatropic rearrangement of **68** to **69** has been studied experimentally[39] and theoretically[40] in some depth. The "symmetry-allowed" path for

68 **69**

the rearrangement should occur via retention of configuration at the migrating methylene carbon. However, the stereochemistry associated with this reaction has unambiguously been shown[39,40] to proceed with inversion of configuration at the migrating carbon. The rearrangements in norcaradiene and η^2-benzene–ML_2 are, therefore, analogous in that they both violate orbital symmetry rules, and they both do so because of superjacent orbital control.[41] We shall not present a detailed comparison of both systems here.[33] For benzene–$Ni(CO)_2$, the leading interactions are given in **70** and **71** for conformations **65** and **66**, respectively. The overlap

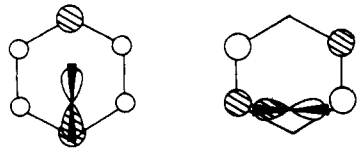

70 **71**

between metal b_1 and the requisite benzene π^* orbital is not identical in each conformation. At the optimized geometry, the overlap in **70** is 0.082, whereas, in **71** it is 0.107.[42] Using perturbation theory considerations,[38c] this overlap difference translates into a 3.4 kcal/mol greater stabilization for two electrons in **71** compared to that in **70**. This is essentially identical with the computed energy difference between **65** and **66** (3.3 kcal/mol).

The failure of Mingos' and our symmetry-based rules to predict the correct stereochemistry in the η^2-benzene–ML_2 haptotropic rearrangement is a unique case. For example, the hypothetical η^2-cyclopentadienyl–$Pt(CO)_2^-$ complex, **72**, contains an equal number of valence electrons. The model again predicts that

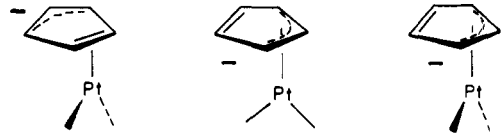

72 **73** **74**

rotation to an η^3 transition state, **73**, should be a lower energy process than sliding to the alternative one, **74**. In computations on this system, we have again lowered the carbon 2s and 2p H_{ii} values on the ring by −3.0 eV for the same reason as in benzene–$Ni(CO)_2$. The optimized structure for **73** was found to be 12.5 kcal/mol lower in energy than **74** which is in agreement with our model.

(38) (a) Hoffmann, R. *Angew. Chem.* **1982**, *94*, 725; *Angew. Chem., Int. Ed. Engl.* **1982**, *21*, 711. (b) Albright, T. A. *Tetrahedron* **1982**, *38* 1339. (c) Albright, T. A.; Burdett, J. K.; Whangbo, M.-H. "Orbital Interactions in Chemistry"; Wiley: New York, 1985; pp 402–421.

(39) (a) For review, see: Klärner, F. G. *Top. Stereochem.* **1984**, *15*, 1. (b) Klärner, F. G.; Brassel, B. *J. Am. Chem. Soc.* **1980**, *102*, 2469. Klärner, F. G. *Angew. Chem.* **1974**, *86*, 270; *Angew. Chem., Int. Ed. Engl.* **1974**, *13*, 268. Klärner, F. G.; Yaslak, S.; Wette, M. *Chem. Ber.* **1979**, *112*, 1168. (c) Baldwin, J. E.; Brolin, B. M. *J. Am. Chem. Soc.* **1982**, *104*, 2857; **1978**, *100*, 4599. (d) Berson, J. A.; Willcott, M. R., III *Ibid.* **1965**, *87*, 2751, 2752; **1966**, *88*, 2494. Berson, J. A.; Grubb, R. W.; Clark, R. A.; Hartter, D. R.; Willcott, M. R., III. *Ibid* **1967**, *89*, 4076.

(40) Schoeller, W. W. *J. Am. Chem. Soc.* **1975**, *97*, 1978.

(41) Berson, J. A.; Salem, L. *J. Am. Chem. Soc.* **1972**, *94*, 8917. Berson, J. A. *Acc. Chem. Res.* **1972**, *5*, 406. Salem, L. In "Chemical and Biochemical Reactivity"; Bergmann, E. D., Pullman, B., Eds.; Israel Academy of Sciences and Humanities: Jerusalem, 1974; pp 329–338.

(42) The reason behind this overlap difference can be traced to the C–C–C angle for the three carbon atoms that are coordinated to Ni. If this angle was 60°, then the two overlaps would be equal, as they are at an η^3 geometry in cyclopropenium–ML_2.[4a] As the C–C–C angle increases, the overlap in **70** decreases and reaches a limiting value at 180°.

Extensions

The molecules that we have covered in the previous sections all have 16-electron η^2 or η^3 geometries. The analysis of haptotropic rearrangements can easily be extended to other electron counts and hapto numbers. Crabtree and co-workers[43] have recently discovered a facile rearrangement shown in **75**. In this

75

76 **77**

compound, the IrL_2^+ fragment is d^8. Referring back to Figure 1, the b_1 ML_2 orbital is the LUMO at this electron count. It then will form the dominant bonding interaction with the HOMO of naphthalene. This is shown in **76**. An obvious, least-motion path for the rearrangement would be for the IrL_2^+ fragment to slide directly under the C_1–C_6 bond. However, one can see from the topology of the naphthalene HOMO that all overlap between it and b_1 must vanish when the IrL_2^+ fragment lies over the bisector of the C_1–C_6 bond. The atomic coefficients at C_2, C_5, C_7, and C_{10} would require an empty metal orbital of δ symmetry to overlap with the naphthalene HOMO at this geometry. A lower energy path will be for the IrL_2^+ fragment to rotate in a clockwise sense and migrate over the C_6–C_7 bond, as shown by the dashed arrow in **76**, yielding **77**. The addition of two electrons to **75** generates a d^{10} naphthalene–ML_2 complex.[44] As in the benzene–ML_2 example, the principal source of bonding stems from the filled b_1 ML_2 orbital and naphthalene LUMO. This is illustrated in **78** for an η^2 geometry. Rearrangement from one η^2 geometry

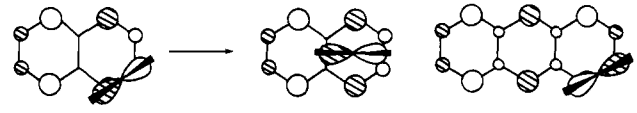

78 **79** **80**

to another within each ring is predicted to be facile via **79**. The motion of the ML_2 from under one ring to the other will be far more difficult. An identical situation occurs for a d^{10} anthracene–ML_2 complex. The interaction of ML_2 b_1 with the LUMO of anthracene is shown in **80**. The ground-state geometry does indeed have this structure;[45] however, nothing has been reported about the dynamics of these compounds.

A system topologically analogous to naphthalene–IrL_2^+ is d^{10} pentalene–PtL_2. The LUMO of pentalene is given in **81**. It is clear that the ground-state geometry should be η^3, **83**. Again

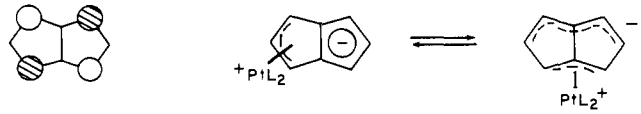

81 **82** **83**

the haptotropic rearrangement of PtL_2 from one ring to the other cannot take place by a least-motion path. It must proceed via **83** for the overlap between b_1 and the pentalene LUMO to be retained. Naphthalene–IrL_2^+ and pentalene–PtL_2 both contain the same number of polyene π plus metal d electrons. A hypo-

(43) Crabtree, R. H., private communications. Crabtree, R. H.; Parnell, C. P. *Organometallics* **1984**, *3*, 1727.

(44) Several examples are known; see: Jonas, K. *J. Organomet. Chem.* **1974**, *78*, 273.

(45) Brauer, D. J.; Krüger, C. *Inorg. Chem.* **1977**, *16*, 884.

Table I. Parameters Used in the Extended Hückel Calculations

orbital	H_{ii}, eV	ζ_1	ζ_2	C_1[a]	C_2[a]
Pt					
5d	−12.38	6.013	2.696	0.6334	0.5513
6s	−8.95	2.554			
6p	−5.38	2.535			
Rh					
4d	−12.50	4.29	1.90	0.5807	0.5685
5s	−8.09	2.14			
5p	−4.57	2.10			
Ni					
3d	−13.44	5.75	2.00	0.5862	0.5845
4s	−9.13	2.10			
4p	−5.12	2.10			
P					
3s	−18.60	1.60			
3p	−14.00	1.60			
C					
2s	−21.40	1.625			
2p	11.40	1.625			
O					
2s	−32.30	2.275			
2p	−14.80	2.275			
H					
1s	−13.60	1.30			

[a] Contraction coefficients used in the double-ζ expansion.

thetical complex with two less electrons is benzocyclobutadiene–FeL_2. The HOMO of benzocyclobutadiene is shown in **84**. The

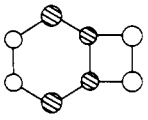

84

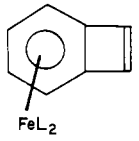

85

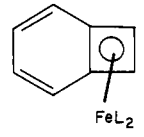

86

empty ML_2 b_1 orbital can overlap substantially with **84** either at an δ^6, **85**, or η^4, **86**, geometry. Because of the nodal structure in **84**, the rearrangement from **85** to **86** should be energetically costly. Butalene–FeL_2, **87**, contains four less electrons than the naphthalene–IrL_2^+ and pentalene–PtL_2 examples. The HOMO of

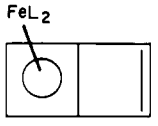

87

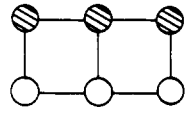

88

butalene is shown in **88**. The haptotropic rearrangement of FeL_2 from one ring to the other is expected to be very facile since overlap between b_1 and **88** can be maintained along a least-motion path.

The alternating facile-difficult activation energies with respect to the number of π plus metal d electrons for haptotropic rearrangements in bicyclic polyene–ML_2 complexes are akin to that found for the ML_3 and MCp systems.[3a] There is, however, no all-encompassing electron-counting rule which can handle all topologies for the ML_2 cases. For example, *trans*-η^4-hexatriene–FeL_2, **89**, contains the same number of π and d electrons as butalene–FeL_2, **87**. Yet the rearrangement from one η^4 geometry

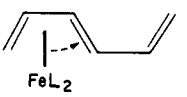

89

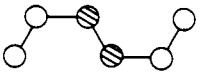

90

to the other, as indicated by the dashed arrow in **89**, will proceed with difficulty. The nodal characteristics of the HOMO in hexatriene, as shown in **90**, will not allow continuous overlap with the b_1 LUMO of FeL_2.[46] Hexatriene–NiL_2, **91**, contains two more electrons. The shift of NiL_2 from one η^2 geometry to another

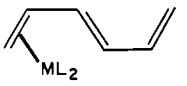

91

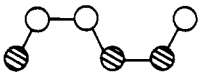

92

will be facile. The NiL_2 b_1 orbital now interacts with the hexatriene LUMO, **92**. Overlap between the two fragment orbitals is retained along a least motion reaction pathway.

Acknowledgment. We thank Bob Crabtree for stimulating discussions, Natalie Mosley for expert typing, and Wendy Puntenney for a skillful rendering of the drawings. Our work was supported in part by the Robert A. Welch Foundation and the Petroleum Research Foundation, administered by the American Chemical Society.

Appendix

The entended Hückel calculations[5] utilized a modified version of the Wolfsberg-Helmholz formula.[47] The parameters listed in Table I were taken from previous work.[4a,10] Idealized geometries for the polyenes were used with C–C = 1.41 Å and C–H = 1.09 Å. For the ML_2 groups, the distances utilized were Pt–P, Ni–P, Ni–C, C–O, Rh–P, and P–H = 2.29, 2.15, 1.82, 1.14, 2.20, and 1.42 Å, respectively. The bond angles in the ML_2 units were set at P–Ni–P, P–Rh–P, P–Pt–P, C–Ni–C, Ni–C–O, and M–P–H = 110.0°, 99.2°, 103.0°, 90.0°, 180.0°, and 123.1°, respectively.

(46) The reader should note that the η^4-to-η^4 rearrangement in a *cis*-hexatriene–FeL_2 or cycloheptatriene–FeL_2 complex will be facile. Overlap between the hexatriene HOMO and b_1 is, in this geometry, retained along a least-motiopn transit.

(47) Ammeter, J. H.; Bürgi, H.-B.; Thibeault, J. C.; Hoffmann, R. *J. Am. Chem. Soc.* **1978**, *100*, 3686.